



# REMOVAL OF TITAN YELLOW DYE FROM AQUEOUS SOLUTION BY POLYANILINE/Fe<sub>3</sub>O<sub>4</sub> NANOCOMPOSITE

Mohamed A. Salem,<sup>[a]\*</sup> Ibrahim A. Salem,<sup>[a]</sup> Mahmoud G. Hanfy,<sup>[b]</sup> and Ahmed B. Zaki<sup>[a]</sup>

**Keywords:** Adsorption, Magnetite, Polyaniline nanocomposites, Titan yellow, wastewater treatment, dye removal

The efficiency of polyaniline/Fe<sub>3</sub>O<sub>4</sub> (PANI/Fe<sub>3</sub>O<sub>4</sub>) nanocomposite (NC) as an adsorbent was investigated in the removal of Titan yellow (TY) dye from aqueous solution. The PANI/Fe<sub>3</sub>O<sub>4</sub> was synthesized by polymerization of aniline in H<sub>2</sub>SO<sub>4</sub> medium in the presence of Fe<sub>3</sub>O<sub>4</sub> nanoparticles with ammonium persulfate as an oxidant. The NC formed was characterized by SEM and FT-IR methods. The dye removal process was studied under various conditions and was found that the adsorption activity of the PANI/Fe<sub>3</sub>O<sub>4</sub> NC was greater than that of the bare PANI and Fe<sub>3</sub>O<sub>4</sub> nanoparticles. Adsorption kinetics fitted with pseudo-first-order kinetic model.

## Corresponding Authors

Fax: +20403350804

E-Mail: masalem@science.tanta.edu.eg

[a] Chemistry Department, Faculty of Science, Tanta University, Tanta 31527, Egypt

[b] West Delta Electricity Production Company, Alex, Egypt

## Introduction

The pollutants in wastewater effluents from industrial sources must be removed or destroyed before water can be discharged into the environment.<sup>1</sup> Textile industry is known to be one of the major sources for the pollution of the environment.<sup>2</sup>

Adsorption is a widely used method for the removal of organic and inorganic pollutants from wastewater effluents,<sup>3</sup> including the removal of dyes from aqueous solutions. The most promising adsorbents of the textile dyes are polyaniline(PANI),<sup>4,5</sup> polyaniline/silica,<sup>6</sup> polyaniline/sawdust,<sup>7</sup> Fe<sub>3</sub>O<sub>4</sub>/C/polyaniline composites,<sup>8</sup> humic acid/Fe<sub>3</sub>O<sub>4</sub>,<sup>9</sup> Fe<sub>3</sub>O<sub>4</sub>/C composites,<sup>10</sup> Fe<sub>3</sub>O<sub>4</sub>/sodium dodecyl sulphate (SDS)<sup>11</sup> and activated carbon.<sup>12,13</sup>

Among the mentioned adsorbents, conducting polymers like PANI and their composites have been the subject of intensive research and development due to their unique properties including their high environmental stability.<sup>14</sup> Aniline polymerization in an aqueous acidic medium yields the most conductive form of PANI, the emeraldine salt (ES), and this can be converted to the corresponding emeraldine base (EB) with an alkaline treatment. The ES and EB are used as excellent adsorbents for both anionic<sup>4</sup> and cationic<sup>6</sup> textile dyes.

The NC of polyaniline with Fe<sub>3</sub>O<sub>4</sub> has received great attention because of its magnetic and electrical properties. It can be prepared via two steps. The first is the preparation of magnetic iron oxide (Fe<sub>3</sub>O<sub>4</sub>) nanoparticles then the second step is polymerization of aniline in the presence of Fe<sub>3</sub>O<sub>4</sub> formed using an oxidant in acidic medium.<sup>15-17</sup>

In the present article, we report the results of the removal of Titan yellow (TY) dye from aqueous solution by PANI/Fe<sub>3</sub>O<sub>4</sub> NC as an adsorbent. The adsorption processes was carried out under controlled reaction conditions to reach the highest removal efficiency.

## Experimental

### Materials

Aniline (Adwic) was distilled twice until it turned colorless. Titan yellow (Figure 1) from Winlab was used without further purification.

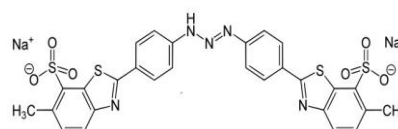


**Figure 1.** Structure of Titan Yellow.

Ammonium peroxydisulfate (APS) (Sigma-Aldrich) was high grade quality and used as received. The measurements were performed in distilled water all over the experimental work.

### Synthesis of oleic acid-coated Fe<sub>3</sub>O<sub>4</sub> nanoparticles

The oleic acid-coated Fe<sub>3</sub>O<sub>4</sub> was prepared by co-precipitation of aqueous Fe<sup>3+</sup>/Fe<sup>2+</sup> ions in the presence of oleic acid (OA). FeCl<sub>3</sub> (14.62 g, 0.09 mol) and FeSO<sub>4</sub>·7H<sub>2</sub>O (12.52 g, 0.045 mol) were dissolved in little amount of water (60 mL), followed by 140 mL water and stirred vigorously at 85 °C. Ammonium hydroxide (50 ml) was added slowly to reach the pH 9. At this stage, oleic acid (4 g) was then added and the reaction was left to continue for 2 h at 50 °C. The black precipitate formed was centrifuged and washed thoroughly with ethanol then water and dried at 60 °C overnight.

## Synthesis of polyaniline (PANI)

Polyaniline in the form of ES was prepared by oxidative polymerization of aniline in aqueous H<sub>2</sub>SO<sub>4</sub> solution in the presence of APS as oxidizing agent. APS (7.5 g, 0.033 mol) and SDS (0.06 g) were transferred into a beaker (500 mL) containing 200 mL of H<sub>2</sub>SO<sub>4</sub> (0.5 M). The mixture was stirred magnetically in an ice bath at 5 °C. Aniline (3 mL, 0.033 mol) was then added dropwise with continuous stirring for 1 h at temperature below 10 °C. The APS/aniline mole ratio was kept at 1:1 in all experiments unless otherwise stated. The deep green precipitate of polyaniline salt was filtered and washed with H<sub>2</sub>SO<sub>4</sub> acid (0.5 M) until the acid filtrate turned colorless. It was further washed with water and dried overnight at 60 °C.

## Synthesis of PANI/Fe<sub>3</sub>O<sub>4</sub> nanocomposite

The nanocomposite was prepared by in situ oxidative polymerization of aniline in the presence of Fe<sub>3</sub>O<sub>4</sub> nanoparticles in an aqueous suspension. Fe<sub>3</sub>O<sub>4</sub> NPs (0.3 g) were dispersed in 200 mL of H<sub>2</sub>SO<sub>4</sub> (0.5 M) and sonicated for 1 h in the presence of SDS (0.06 g). APS (7.5 g, 0.033 mol) was then added and the mixture was stirred continuously at 5 °C followed by the slow addition of aniline (3 mL, 0.033 mol). The polymerization reaction was allowed to proceed under these conditions for 1 h until a dark precipitate of PANI/Fe<sub>3</sub>O<sub>4</sub> NC was obtained. The NC was collected by filtration and washed with the acid solution (0.5 M) until the acid filtrate turned colorless. The product was further washed with large amount of distilled water until the filtrate became colorless. It was dried in oven at 60 °C overnight and the yield was weighed.

## Characterization techniques

Characterization of above samples was performed by conventional techniques. The morphology of samples was studied by the scanning electron microscope (SEM) (JSM, JEOL, 5300). FT-IR measurements were recorded on Jasco FT-IR 4100 (Japan) in the range 4000 – 400 cm<sup>-1</sup>.

X-ray diffraction (XRD) patterns beam was nickel - filtered CuKα ( $\lambda = 1.5405 \text{ \AA}$ ) radiation operated at 40 kV and 30 mA. The scanning range was from  $2\theta = 0$  to  $90^\circ$  with rate of  $2.4^\circ/\text{min}$ .

The UV/Vis spectra were recorded on the UV/Vis spectrophotometer (T80PG instruments ltd) linked with a temperature control unit to adjust the cell holder temperature to the desired value  $\pm 0.1^\circ\text{C}$ .

The thermogravimetric analysis (TGA) technique was used primarily to determine the thermal properties of the prepared NC (SDT Q600 V20.5 Build 15). The technique can analyze materials that exhibit either mass loss due to decomposition, oxidation or loss of volatiles (such as moisture).

The PANI/Fe<sub>3</sub>O<sub>4</sub> composite (0.02 g) was transferred into a conical flask (100 ml) containing 20 ml of the dye solution at 30 °C. The mixture was stirred at 120 rpm. The initial concentration of the dye was varied from 17 to 44 mg L<sup>-1</sup>.

## Results and Discussion

### Transmission electron microscopy (TEM)

The TEM image of the OA-Fe<sub>3</sub>O<sub>4</sub> nanoparticles is shown in (Figure 2c). Spherical nanoparticles of OA-Fe<sub>3</sub>O<sub>4</sub> with average diameter about 12 nm are observed. Figure 2d indicated that the encapsulated OA-Fe<sub>3</sub>O<sub>4</sub> nanoparticles in PANI have average diameter 14 nm.

### Scanning electron microscopy (SEM)

(Figure 2a) shows the SEM micrograph of the free Fe<sub>3</sub>O<sub>4</sub> nanoparticles. The nanoparticles seen to be aggregated in an irregular shape due to their high surface energy. Different appearance was observed in (Figure 2b) for the PANI/Fe<sub>3</sub>O<sub>4</sub>. The nanoparticles of composite bind with PANI-chains to form multiparticles aggregates, which keep the free Fe<sub>3</sub>O<sub>4</sub> nanoparticles tightly bound.

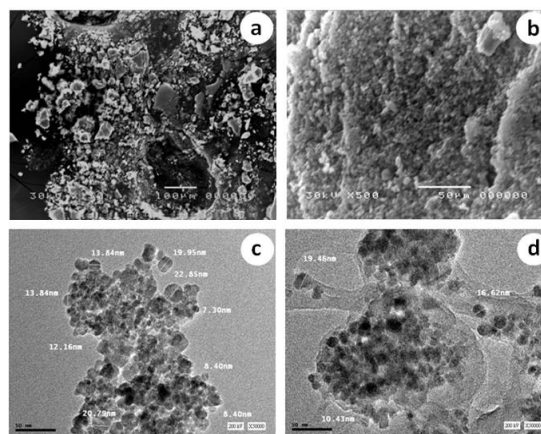


**Figure 2.** SEM images: (a) Oleic acid/Fe<sub>3</sub>O<sub>4</sub>, (b) PANI/OA-Fe<sub>3</sub>O<sub>4</sub>; TEM images: (c) Oleic acid/Fe<sub>3</sub>O<sub>4</sub>, (d) PANI/OA-Fe<sub>3</sub>O<sub>4</sub>.

### FT-IR

The FT-IR spectrum of Fe<sub>3</sub>O<sub>4</sub> nanoparticles (Supplementary material, S1) shows a band at 3429 cm<sup>-1</sup>, which is a characteristic of the free OH groups on the nanoparticle surface. The peaks at 2924 cm<sup>-1</sup> and 2854 cm<sup>-1</sup> correspond to the stretching vibration of saturated –C–H groups due to the oleic ester. The stretching vibration of C=O of oleic acid is at 1703 cm<sup>-1</sup>. The peaks at 587 cm<sup>-1</sup> and 451 cm<sup>-1</sup> are assigned to the vibration of Fe<sup>2+</sup>-O and Fe<sup>3+</sup>-O bonds, respectively. The band at 1102 cm<sup>-1</sup> is assigned to the C–N bonds, while the peak at 3231 cm<sup>-1</sup> corresponds to the N–H stretching vibration.

The PANI/OA-Fe<sub>3</sub>O<sub>4</sub> nanoparticles formation is attributed to the strong interaction between PANI and OA-Fe<sub>3</sub>O<sub>4</sub>. Iron has the capability to form coordination bonds with the –NH group of PANI chain.<sup>16,18</sup> and hydrogen bond can also be formed between the O atom of the carbonyl group of OA-Fe<sub>3</sub>O<sub>4</sub> and the –NH of PANI. Hydrogen bonds may also be formed between the hydroxyl group at the surface of OA-Fe<sub>3</sub>O<sub>4</sub> and N atom of the quinonoid structure (peaks at 1565 cm<sup>-1</sup> and 1444 cm<sup>-1</sup> are assigned to quinonoid and benzenoid structures, respectively).

### X-ray diffraction

Figure 3 shows the XRD pattern of OA-Fe<sub>3</sub>O<sub>4</sub> nanoparticles and PANI/Fe<sub>3</sub>O<sub>4</sub> NC. A comparison between both the patterns revealed that a single peak at  $\theta = 25^\circ$  appears in the PANI/Fe<sub>3</sub>O<sub>4</sub>, which is characteristics of the PANI. The rest of peaks are assigned to the OA-Fe<sub>3</sub>O<sub>4</sub> which has a cubic crystal system. These results agree with the reported results.<sup>19</sup> Crystallite size of magnetic nanoparticles is calculated from Scherrer equation.<sup>20,21</sup> The average size of the Fe<sub>3</sub>O<sub>4</sub> particles is found to be 8 - 10 nm which is consistent with the results of TEM.

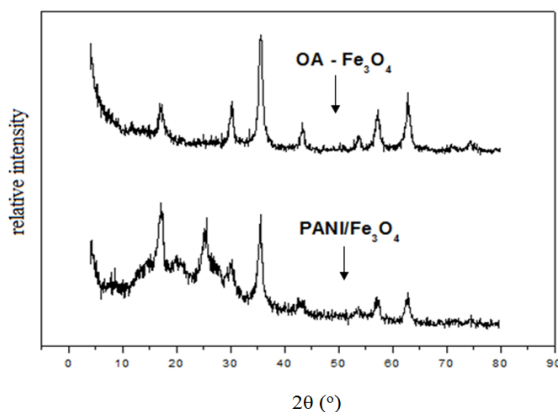


**Figure 3.** XRD patterns of OA-Fe<sub>3</sub>O<sub>4</sub> and PANI/ OA-Fe<sub>3</sub>O<sub>4</sub>.

### Adsorption of TY on PANI/Fe<sub>3</sub>O<sub>4</sub>

On the addition of the dye solution to the NC sample, a relative fast decolourization took place (Figure 4). The absorbance of the dye solution decreased by ca. 80 % over 90 min, depending on the operating reaction conditions. Adsorption of TY onto the bare Fe<sub>3</sub>O<sub>4</sub>, PANI and the NC was also investigated. The rate constant of dye adsorption from solution follows the order PANI/Fe<sub>3</sub>O<sub>4</sub> > Fe<sub>3</sub>O<sub>4</sub> > PANI under similar conditions. Adsorption of the dye by PANI occurred due to the electrostatic interactions between the -NH<sup>+</sup>- centers of PANI (ES form) and dye anions. The difference between the amount of the dye adsorbed on Fe<sub>3</sub>O<sub>4</sub> nanoparticles and PANI/Fe<sub>3</sub>O<sub>4</sub> NC illustrates the presence of active sites for TY adsorption. The increase in the functional O and N atom containing groups content in the NC comparing that in bare Fe<sub>3</sub>O<sub>4</sub> makes the NC to be desirable for dye adsorption.<sup>22</sup> The results obtained may be explained in terms of the increasing the amount of this groups and the surface area of the PANI/Fe<sub>3</sub>O<sub>4</sub> NC.

### Effect of PANI/Fe<sub>3</sub>O<sub>4</sub> NC and dye concentrations

The rate of adsorption increased with increasing the NC amount. This can be explained in terms of the availability of active sites on the PANI/Fe<sub>3</sub>O<sub>4</sub> surface that is eligible to interact with the TY molecules. The effect of dye concentration on the rate of reaction was investigated by keeping the amount of PANI/Fe<sub>3</sub>O<sub>4</sub> constant and the dye concentration varies in the range (0.5 - 1.5) × 10<sup>-4</sup> M. The rate of adsorption decreases with an increase in the dye concentration.

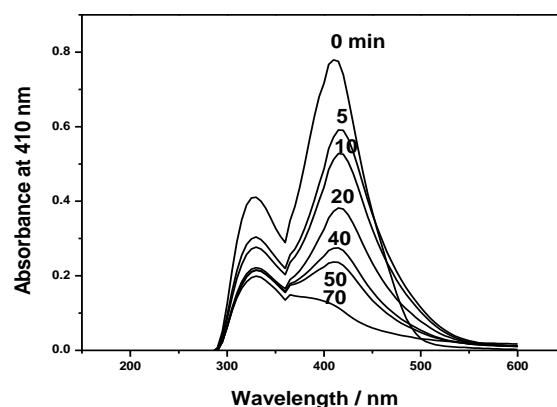


**Figure 4.** Absorbance traces of TY with time in the presence of PANI/OA-Fe<sub>3</sub>O<sub>4</sub> [TY] = 2.6 × 10<sup>-4</sup> mol L<sup>-1</sup>, PANI/OA-Fe<sub>3</sub>O<sub>4</sub> = 0.02 g.

The more dye concentration the greater loading of NC surface with dye molecules are occurred. A slower adsorption would then be expected with the continuous blocking of the available active sites on the NC surface with the previously adsorbed molecules of the dye.

### Effect of pH

The rate of dye removal by adsorption on the NC depends greatly on the pH of the medium. The measurement of the rate was carried out in the pH range 2-8 using phosphate buffer. The rate constant decreased with increasing the pH of from 2 to 8 (Figure 5). In strong acidic medium, the PANI always exists in the form of ES. This form is rich with the positively charged sites that undergo interaction with anionic moiety of the dye molecule. The ES form transforms into the EB form at higher pH. As the pH increases, the transition continues leading to the depletion of active sites in the polymer skeleton and consequently the interaction of PANI with TY is inhibited.

### Adsorption kinetics

The effect of the initial dye concentration on the adsorption parameters was studied. The amount of dye adsorbed,  $q_t$  (mg g<sup>-1</sup>), at time  $t$  for each concentration was estimated by the mass balance equation.

$$q_t = V \frac{C_0 - C_t}{m} \quad (1)$$

where

$C_0$  is the initial concentration (mg L<sup>-1</sup>) of TY,

$C_t$  is the concentration of the remaining dye in solution at time  $t$  (mg L<sup>-1</sup>),

$V$  is the total volume (L) of reaction mixture and

$m$  is the mass in gram of PANI/Fe<sub>3</sub>O<sub>4</sub> sample.

The  $q_t$  increased with the contact time of the dye with the adsorbent and also with the initial concentration of the dye. The dye adsorption on PANI/Fe<sub>3</sub>O<sub>4</sub> was initially fast and then slowed down thereafter.

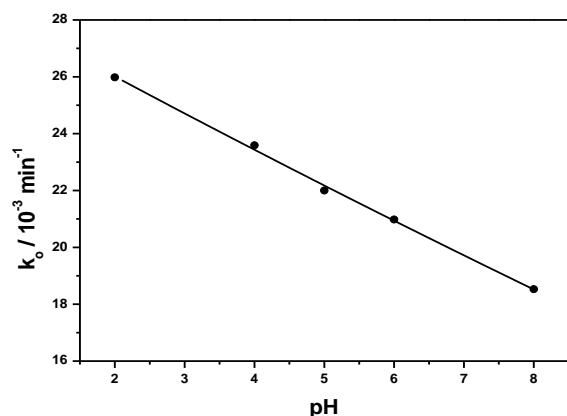


**Figure 5.** The dependence of the rate constant upon the pH. PANI/OA-Fe<sub>3</sub>O<sub>4</sub> = 0.02 g, [TY] =  $2.6 \times 10^{-4}$  mol L<sup>-1</sup>, T = 30°C.

The adsorption kinetic data were analyzed in terms of different types of mathematical models. The first is pseudo-first-order kinetic model proposed by Lagergren's<sup>23</sup> in eqn. (2).

$$\log(q_e - q_t) = \log q_e - t \quad (2)$$

where

$q_t$  and  $q_e$  (mg g<sup>-1</sup>) are the amounts of dye adsorbed per unit mass of the NC at time  $t$  and at equilibrium, respectively.

$k_1$  (min<sup>-1</sup>) is the pseudo-first-order rate constant of adsorption.

Figure 6 shows the linear relationship between  $\log(q_e - q_t)$  and  $t$ . The slope of the plot is  $k_1$  and the intercept is  $\log(q_e)$ .

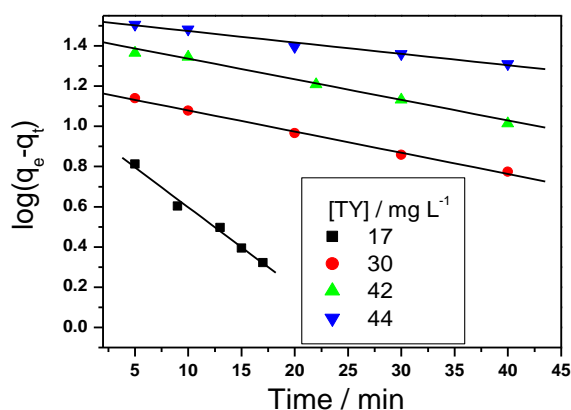


**Figure 6.** Pseudo-first-order kinetics for adsorption of TY onto PANI/OA-Fe<sub>3</sub>O<sub>4</sub>. PANI/OA-Fe<sub>3</sub>O<sub>4</sub> = 0.02 g, T = 30°C.

The second model is pseudo-second-order kinetic, proposed by Ho and McKay<sup>24</sup> which is represented by the equation,

$$\frac{t}{q_t} = \frac{1}{k_2 q_e^2} + \frac{t}{q_e} \quad (3)$$

where

$q_e$  is the amount of dye adsorbed at equilibrium (mg g<sup>-1</sup>), and

$k_2$  is pseudo-second-order rate constant for adsorption (g mg<sup>-1</sup> min<sup>-1</sup>).

$k_2 q_e^2$  is the initial rate of adsorption at  $t \rightarrow 0$ .

Values of  $q_e$ ,  $k_2 q_e^2$  and  $k_2$  are calculated from the slope and intercept of the straight line obtained from the plot  $t/q_t$  vs  $t$  at various dye concentrations. Values of  $k$  and  $q_e$ , and correlation coefficient for this kinetic model are given in Table 1. Because of the correlation coefficients obtained for pseudo-first-order kinetic model are higher than for pseudo-second-order models, then the adsorption process follows better the former one.

**Table 1.** Kinetic parameters for adsorption of TY onto PANI/Fe<sub>3</sub>O<sub>4</sub> NC

Kinetic models and parameters	C <sub>0</sub> of TY (mg L <sup>-1</sup> )			
	17	30	42	44
$q_e$ (exp), mg g <sup>-1</sup>	12	20	30	34
<b>Pseudo-first-order</b>				
$q_e$ (calcd.), mg g <sup>-1</sup>	10	18	28	34
$k_1$ , min <sup>-1</sup>	0.0915	0.0243	0.0236	0.013
$R^2$	0.993	0.998	0.992	0.992
<b>Pseudo-second-order</b>				
$q_e$ (calcd.), mg g <sup>-1</sup>	15	21	26	56
$k_2 \times 10^{-3}$ , g mg <sup>-1</sup> min <sup>-1</sup>	9.3	5.4	2.6	14
$R^2$	0.998	0.996	0.964	0.980

### Adsorption isotherms

The Langmuir and Freundlich isotherm models were applied to estimate the adsorption capacity of the PANI/Fe<sub>3</sub>O<sub>4</sub> NC towards the TY in view of the adsorption results obtained.

### Langmuir adsorption isotherm

The following equation describes the monolayer surface coverage of the NC with the adsorbed dye molecules.<sup>25</sup>

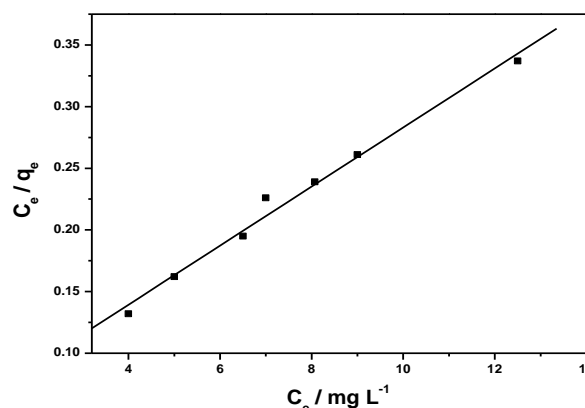


**Figure 7.** Langmuir isotherm for adsorption of TY on PANI/OA-Fe<sub>3</sub>O<sub>4</sub>. PANI/OA-Fe<sub>3</sub>O<sub>4</sub> = 0.02 g, T = 30° C



**Table 2.** Isotherms constants for the adsorption of TY onto PANI/ Fe<sub>3</sub>O<sub>4</sub> PANI/Fe<sub>3</sub>O<sub>4</sub> = 0.02 g, Temp = 30 °C.

Langmuir isotherm parameters				Freundlich isotherm parameters			
$q_m$	$K_L$	$R_L$ range	$R^2$	$K_F$	$1/n$	$n$	$R^2$
50	0.415	0.12–0.05	0.998	3.8	0.86	1.16	0.997

$$\frac{C_e}{q_e} = \frac{C_e}{q_m} + \frac{1}{q_m K_L} \quad (4)$$

where,

$q_e$  is the amount of dye adsorbed at equilibrium (mg g<sup>-1</sup>)

$C_e$  is the equilibrium concentration of the dye (mg L<sup>-1</sup>) in bulk solution.

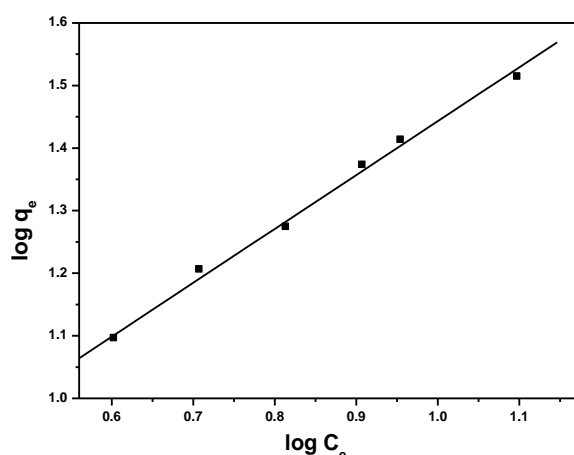
$K_L$  is the equilibrium constant (L g<sup>-1</sup>) while

$q_m$  represents the maximum adsorption capacity when one layer of dye molecules is completed on the surface of the NC.

$K_L$  and  $q_m$  are derived from the intercept and slope of  $C_e/q_e$  versus  $C_e$  plot which is shown in (Figure 7). It is known that the Langmuir isotherm is related to a dimensionless separation factor  $R_L$  that is defined as

$$R_L = \frac{1}{1 + K_L C_s} \quad (5)$$

The  $R_L$  denotes to the state of the adsorption process. If ( $0 < R_L < 1$ ) the adsorption is favorable, ( $R_L > 1$ ) it is unfavorable, ( $R_L = 1$ ) is linear, and ( $R_L = 0$ ) is irreversible.

**Figure 8.** Freundlich isotherm for adsorption of TY on PANI/OA-Fe<sub>3</sub>O<sub>4</sub>. PANI/OA-Fe<sub>3</sub>O<sub>4</sub> = 0.02 g,  $T = 30^\circ\text{C}$ .

In the present study the value of  $R_L$  is ranging from 0.12 to 0.05 for the different initial concentrations of TY used. Table 2 indicates a favorable adsorption of the dye by PANI/Fe<sub>3</sub>O<sub>4</sub> NC.

### Freundlich adsorption isotherm

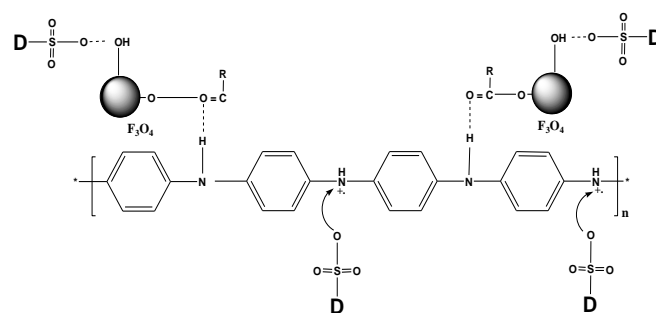
Freundlich model is given by the eqn. (7).<sup>26</sup>

$$\log q_e = \log K_F + (1/n) \log C_e \quad (6)$$

Values of  $K_F$  and  $n$  denote to the adsorption capacity and adsorption intensity, respectively. They were calculated from the intercept and the slope of the  $\log q_e$  vs  $\log C_e$  plot (Figure 8).  $1/n$  describes the heterogeneity in adsorbent surface. Its small value indicates a favorable. A value close to or equals 1 indicates a material with relatively homogenous binding sites. A high value of  $K_F$  confirms a high adsorption capacity of the adsorbent. Adsorption isotherms of both Langmuir and Freundlich are depicted in (Figures 7, 8). The adsorption parameters derived from these isotherms are summarized in Table 2. The correlation coefficients ( $R^2$ ) confirm that both isotherms are satisfactory.

### Adsorption mechanism

The possible proposed adsorption mechanism of the dye on the surface of PANI/Fe<sub>3</sub>O<sub>4</sub> involves two routes. The first is the electrostatic interaction between the dye molecules and the polyaniline salt. The second is the formation of a coordination bond between Fe<sub>3</sub>O<sub>4</sub> and the dye as shown in Figure 9.

**Figure 9.** Adsorption mechanism between PANI/Fe<sub>3</sub>O<sub>4</sub> NC and TY.

On dissolution of the dye in water it dissociates into dye anions ( $\text{D-SO}_3^-$ ) and  $\text{Na}^+$  ions, where D denotes to the organic moiety of the dye molecule. This anion interacts with the positive centres ( $-\text{NH}^+-$ ) on the PANI surface. The effect of pH given (Fig. 5) is a good evidence for this phenomena. In acidic medium the adsorption is great due to the existence of more  $-\text{NH}^+-$  species on the PANI skeleton. In the basic medium the concentration of these species decreases and therefore the interaction between the adsorbent and the adsorbate is declined.

Regarding the participation of Fe<sub>3</sub>O<sub>4</sub> in the adsorption process, it may be attributed to the development of a bond between the Fe<sub>3</sub>O<sub>4</sub> and the dye molecule.

## Conclusion

Adsorption of TY dye is more efficient onto the PANI/Fe<sub>3</sub>O<sub>4</sub> NC compared with the bare PANI and Fe<sub>3</sub>O<sub>4</sub>. It obeyed both the Langmuir and Freundlich adsorption isotherms. The adsorption process was spontaneous and followed pseudo-first-order kinetic model. This method is promising towards the treatment of wastewater containing dyes.

## References

- <sup>1</sup>Ghasemzadeh, G., Momenpour, M., Omid, F., Hosseini, M. R., Ahani, M., Barzegari A., *Front. Environ. Sci. Eng.*, **2014**, 8, 471.
- <sup>2</sup>Cerge, V. K., Kumar, R., Gupta, R., *Dyes Pigment*, **2004**, 62, 1.
- <sup>3</sup>Juang, R., Tseng, R., *Colloids and Surf. A*, **2002**, 201, 191.
- <sup>4</sup>Salem, M. A., *Reactive & Functional Polymers*, **2010**, 70, 707.
- <sup>5</sup>Ayad, M. M., El-Hefnawy, G., Zaghlool, S., *Chem. Eng.*, **2013**, 217, 460.
- <sup>6</sup>Ayad, M. M., Abu El-Nasr, A., Stejskal, J., *Indus. Eng. Chem.*, **2012**, 18, 1964.
- <sup>7</sup>Ansari, R., Dezhampannah, H., *Eur. Chem. Bull.*, **2013**, 2(4), 220.
- <sup>8</sup>Yao, W., Shen, C., Lu, Y., *Composite Sci. Technol.*, **2013**, 87, 8.
- <sup>9</sup>Zhang, X., Wu, P., Zhang, L., Zeng G., Zhou C., *Colloids Surf. A*, **2013**, 435, 85.
- <sup>10</sup>Zhang, Z., Kong, J., *J. Hazard. Mat.*, **2011**, 139, 325.
- <sup>11</sup>Shariati, S., Faraji, M., Yamini, Y., Rajabi, A., *Desalination*, **2011**, 270, 160.
- <sup>12</sup>Gupta, V. K., *Environ. Manag.*, **2009**, 90, 2313.
- <sup>13</sup>Kumar, P. S., Ramalingam, S., Sathishkumar, K., *Korean J. Chem. Eng.*, **2011**, 28, 149.
- <sup>14</sup>Quadrat, O., Stejskal, J., Kratochvil, P., Kubát, J., Sába, P., McQueen, D., *Synth. Met.*, **1998**, 97, 37.
- <sup>15</sup>Guo, H., Zhu, H., Lin, H., Zhang, J., *Mater. Lett.*, **2008**, 62, 2196.
- <sup>16</sup>Wang, H., Wang, R., Wang, L., Tian, X., *Colloids Surface A*, **2011**, 384, 624.
- <sup>17</sup>Tamilarasan, P., Ramaprabhu, S., *Int. J. Greenhouse Gas Control*, **2012**, 10, 486.
- <sup>18</sup>Deng, J., Ding, X., Zhang, W., Peng, Y., Wang, J., Long, X., *Polymer*, **2002**, 43, 2179.
- <sup>19</sup>Iton, H., Sugimoto, T., *J. Colloid. Interf. Sci.*, **2003**, 265, 283.
- <sup>20</sup>Gass, J., Poddar, P., Almand, J., Srinath, S., Srikanth, H., *Adv. Funct. Mater.*, **2006**, 16, 71.
- <sup>21</sup>Wang X., Chen, X., Ma, X., Zhang, Z., Zhang, Z., *Chem. Phys. Lett.*, **2004**, 384, 391.
- <sup>22</sup>Illés, E., Tombácz, E., *Colloid Surf. A*, **2003**, 230, 99.
- <sup>23</sup>Lagergren, S., *Kung. Sven. Vetenskapsak. Handl.*, **1898**, 24, 1.
- <sup>24</sup>Ho, Y.S., Mckey, G., *process biochem.*, **2009**, 34, 451.
- <sup>25</sup>Langmuir, I., *J. Am. Chem. Soc.*, **1918**, 40, 1361.
- <sup>26</sup>Freundlich, H. M. F., *J. Phys. Chem.*, **1906**, 57A, 385.

Received: 04.04.2016.  
Accepted: 21.05.2016.